Design of a GaN Based Integrated Modular Motor Drive

M. Uğur, O. Keysan

***Abstract* -- In this study, design procedure of an Integrated Modular Motor Drive (IMMD) is presented focusing on having power density. The design is based on a permanent magnet synchronous motor (PMSM) and GaN FETs. Suitable slot/pole combinations and winding configurations are discussed in order to reduce the space harmonics on the motor. An extended motor drive inverter topology is proposed where 2-level voltage source inverters are connected both in series and parallel. Optimum selection of number of modules is achieved and device selection is performed based on loss characterization. Selection of optimum DC link capacitor bank is performed and the effect of interleaving is investigated. The performance of the motor is validated with ANSYS/Maxwell simulations. Motor drive performance is obtained with MATLAB/Simulink simulations. The efficiency of the motor drive is enhanced by 2% compared to a conventional motor drive. A motor drive power density of 15 kW/lt has been achieved.**

***Index Terms*—Gallium Nitride, Integrated motor drive, Modular motor, Permanent magnet synchronous motor, Power Density**

I. Introduction

In conventional motor drive systems, the drive units are placed in separate cabinets which increases the overall weight and volume and decreases the power density of the system. Furthermore, the drive units are connected to the motor by means of long cables which cause transient voltage overshoots due to the high frequency pulse width modulation (PWM) operation.

A novel concept called Integrated Modular Motor Drives (IMMDs) has been proposed in the last few years suggesting that all the components of the motor drive system can be integrated onto the motor including power electronics, control electronics, passive components and heat sink [1]. By doing so, the power density of the system can be enhanced significantly which is very critical in aerospace and electric traction applications [2], [3]. In addition to that, cost reduction up to 20% is possible thanks to the elimination of enclosures and connection equipment [1]. The absence of connection cables yields less leakage current on the winding insulation which will extend the lifespan of the motor as well as minimize electromagnetic interference (EMI) problems [4].

With modularization, the overall system is segmented with modules sharing the total power equally. By this way, the fault tolerance of the system is increased [2]. The current and voltage stress on the power semiconductor devices can also be decreased by modularization. Moreover, the components which produce heat due to power loss are spread and distributed in a wider surface area which makes the thermal design more convenient as well as decreases the possibility of hot spot formation. Finally, the manufacturing, installation and maintenance costs decrease thanks to the modular structure [1].

However, integration of the motor and drive brings several challenges. First, fitting all the drive components to the available space requires size optimization and careful layout design [4]. Second, it is difficult to cool the motor and drive simultaneously since they both produce heat. Furthermore, all the electronic components are subjected to a higher ambient temperature and continuous vibration and should be selected accordingly [5].

To overcome these challenges, it has been proposed in the literature that wide band gap (WBG) power semiconductor devices such as Gallium Nitride (GaN) can be used which are capable of operating at high frequencies [4]. By doing so, the size of the passive components can be reduced with acceptable heat sink size thanks to superior efficiency of GaN based converters compared to conventional ones [6]. However, high frequency operation highlights the parasitic components on the power stage and gate drive circuits which makes layout design critical.

In this paper, design of an IMMD system is presented with enhanced power density, increased efficiency and enhanced fault tolerance capability. A detailed design procedure is given for both motor and the drive and the resultant design parameters are verified using ANSYS/Maxwell and MATLAB/Simulink simulations. Comparison of the IMMD performance with a conventional counterpart having IGBTs is also provided. In Section 2, basic structure and current technology prospects of IMMDs are introduced. In section 3, design of the system including the motor and the drive is explained. In section 4, simulation results are presented and in section 5, conclusions are given.

II. Basic Structure of IMMD

There are several types of integration of the motor drive onto the motor. In this paper, integration into the stator back iron is considered, which also allows the modularization of the system. In this configuration, one module is composed of a

This work was supported by the Scientific and Technological Research Council of Turkey (TUBITAK) under the TUBITAK project number 117E252.

Mesut Uğur is with the Department of electrical and electronics Engineering, Middle East Technical University, Ankara, 06800, TURKEY (e-mail: mesut.ugur@metu.edu.tr).

Ozan Keysan is with the Department of electrical and electronics Engineering, Middle East Technical University, Ankara, 06800, TURKEY (e-mail: keysan@metu.edu.tr).

stator pole piece, a concentrated coil and a power converter dedicated to its own winding along with its controller [5]. Two prototype examples of such a structure from the literature are shown in Fig. 1 [4], [7].

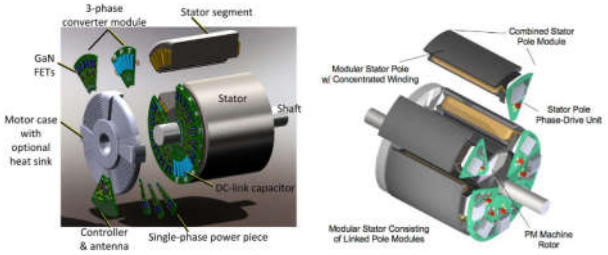

Fig. 1. IMMD prototype examples with stator back-iron integration [4], [7]

In conventional (non-modular) motors, each stator winding belonging to different pole pairs on the stator are usually connected in series to form one phase of the stator. On the other hand, the windings in different poles can be connected to separate motor drive units in modular motors. These types of motors are also called split-winding machines [8], as the redundancy and fault tolerance of the system is enhanced thanks to this modularization. Moreover, the motor drive modules can be connected with different configurations which makes the design more flexible.

A general block diagram of one module of an IMMD system is shown in Fig. 2 [5]. On the machine pole, concentrated windings are preferred for their easy manufacturing and suitability for split-winding stators, especially in modular motors. Fractional slot concentrated winding (FSCW) permanent magnet synchronous motors (PMSMs) are very common in IMMD studies thanks to their high torque density, low torque ripple and fault tolerance capability [9].

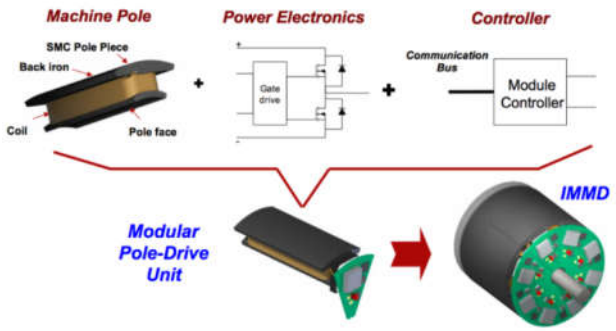

Fig. 2. General block diagram of one module of an IMMD [5]

As for the power electronics, many different topologies have been proposed for AC motor drive systems such as, 2-level voltage source inverter (VSI), multilevel neutral point clamped (NPC) VSI, multilevel flying capacitor (FC) VSI, cascaded H-bridge (CHB) etc. [8]. As mentioned previously, for a modular motor drive, several other motor drive topologies become available thanks to the design flexibility. Connection of separate 2-level VSIs in series or parallel are shown in Fig. 3, with a conventional motor drive [10]. Furthermore, the aforementioned topologies can also be connected in series and/or parallel on the DC link to form a new topology. These types of connections are possible thanks to the fact that the windings, which are split and hence electrically isolated, do not cause in-circulating currents among the inverter modules. The major advantage of this possibility is to be able to split the voltage and/or current requirement of each inverter. One practical usage of this fact is the availability of low voltage power semiconductor device utilization such as GaN in case of high DC link voltage.

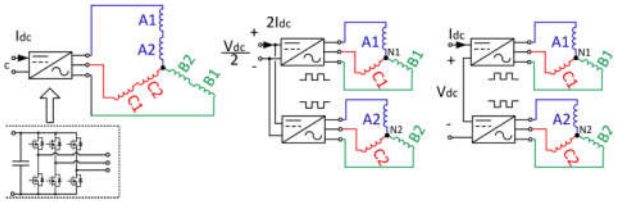

(a) Conventional (b) Parallel (c) Series

Fig. 3. Different motor drive connections for a modular motor [10]

The employment of GaN devices is especially crucial for IMMDs because these devices are one of the so-called WBG type semiconductor devices. These devices have much higher switching speeds compared to conventional silicon based devices such as IGBTs and admissible on-state losses which make them more efficient [11]. Moreover, they have higher maximum junction temperatures. The volume reduction challenge of integrated motor drives can be addressed by the utilization of GaNs thanks to higher efficiency which makes cooling easier, and their fast switching speed which enables high switching frequencies reducing the size of passive components. In high power applications, the maximum switching frequency which can be applied to an IGBT is limited to 20 kHz, whereas GaNs can be used with frequencies as high as 100 kHz in applications with kW range [11]. As a matter of fact, while IGBTs were firstly used in previous IMMD prototypes [5], [7], latest IMMD prototypes utilize GaNs FETs as power semiconductor device [4].

Selection of DC bus capacitors is also very critical in integrated drives in terms of power density as they usually constitute more than 20% of the system volume and 30% of the system weight [6]. Moreover, the height of the motor drive is mostly determined by these capacitors [4]. In conventional motor drives, aluminum electrolytic type capacitors are mostly used thanks to their low cost and high capacitance per volume. However, they have low RMS current handling capability per unit volume and they have relatively shorter lifetime which is also dependent on the operating parameters [6]. On the other hand, metal film type capacitors are a better choice in terms of RMS current ratings, lifetime and reliability. It is also possible to significantly reduce the size of the capacitor bank if required capacitance can be decreased somehow. Therefore, metallized polypropylene film capacitors are most common types in the DC bus of integrated drives.

III. DESIGN OF THE IMMD SYSTEM

The design process of the IMMD system can be considered in two-fold: design of the motor and design of the drive. The first assumption in the design process is that the motor drive input is a passive diode bridge rectifier with an LC DC link pre-filter. The effects of this rectifier module on the rest of the system are kept out of the scope of this study. The machine is a 3-phase low speed PMSM having a modular stator with fractional slot concentrated winding. The system parameters used in the design process are shown in Table 1.

The first parameter to be decided is the total number of 2-level VSI modules. As stated before, the number of series or parallel connected modules can be varied according to the voltage and current requirements and the system parameters such as the DC link voltage and total output power. It has also been specified that GaN transistors will be used to reach the efficiency aim and meet the volume reduction challenge. Blocking voltage rating of the current commercial GaN transistors is 650V at most [11]. When 2L-VSIs are used, the minimum power semiconductor blocking voltage rating in this design is 810V. This value is calculated based on a safety margin considering the voltage overshoot effects due to parasitic inductances and high switching speed, and possible swell or overvoltage events on the grid side. It is clear that, at least two series modules should be used with the aforementioned GaN devices. This also makes the total number of modules an even number.

There are various parameters which affect the number of parallel connected modules. One of them is the required power rating of each module which effect the current ratings of the semiconductor devices and drive efficiency. Another one is the number of stator slots. Instead of number of stator slots per pole per phase (q_s) which has been used in conventional systems, a new parameter, number of stator slots per module per phase (w_s) is defined in this paper. For a double layer stator, w_s can be selected as the multiples of 2. As an example, for an IMMD having 2 series and 3 parallel modules, and stator slots per module per phase is 2, the number of stator slots (Q_s) turns out to be 36. Finally, the effect of interleaving and its utilization for minimization of DC link capacitor bank size is considered to determine the number of modules. In [6], the effect of the number of modules and applied interleaving angle to the current ripple on the DC link capacitor bank is studied for an IMMD, and it has been shown that selecting four modules yields best results in terms of DC link capacitor size. Using that result, it is decided to use a total number of 4 modules which are connected in 2-series and 2-parallel configuration. The schematic diagram of the suggested IMMD system topology is shown in Fig. 4.

TABLE I
THE SYSTEM PARAMETERS USED IN THE IMMD DESIGN PROCESS

Parameter	Value
DC link voltage, V_{dc}	540 V
Total output power, P_{out}	8 kW
Motor efficiency aim, $\eta_{m,a}$	94%
Drive efficiency aim, $\eta_{d,a}$	98%
Rated speed, N_r	600 rpm

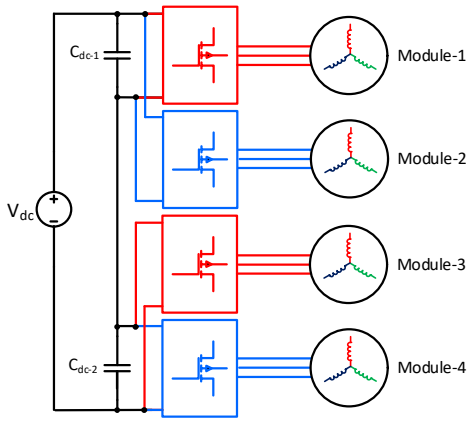

Fig. 4. Schematic diagram of the suggested IMMD topology with 2-series and 2-parallel 2-level VSIs

A. Design of the Motor Parameters

The main dimensions of the motor are determined according to the torque requirement (T_m) and shear stress (σ) using magnetic loading (B) and electrical loading (A) limits selected for the IMMD application, as expressed in (1). V_m stands for the motor air gap volume which is shown in (2), where D_{is} is the air gap (bore) diameter and L_a is the axial length of the motor. The aspect ratio, which is the ratio of the axial length to the bore diameter is selected as 0.5 for this application. The number of slots should be an integer multiple of 24 since the number of 3-phase modules is 4. For the given dimensions, increasing the number of slots per module per phase makes the outer diameter too large. It has been observed that better results in terms of copper fill factor are achieved when w_s is 2. Moreover, the number of rotor poles is selected as 20 by using previously obtained winding factor tables for different slot/pole combinations [9].

The number of turns per coil side can be determined by the induced voltage requirement of each phase on each module, which can be expressed as in (3), in rms, where $N_{ph\text{-}m}$ is number of turns per phase per module, f_s is the applied fundamental frequency at rated conditions, Φ_{pp} is the flux under a pole and k_w is the fundamental winding factor. The flux per pole can be calculated using the machine dimensions and air gap flux density (B_g) as in (4), where p is the number of rotor poles. The winding factor is determined using the pre-calculated tables created for fractional slot machines in terms of slot/pole combinations as 0.933 [9]. The fundamental frequency is also determined by the rated speed and pole number of the synchronous motor, as in (5). Assuming that the motor drive inverters are switched with sinusoidal pulse width modulation (SPWM) technique, the terminal voltage of one phase of each module is determined using (6), where m_a is the modulation depth and $V_{dc\text{-}m}$ is the nominal DC link voltage on one module. The required number of turns per coil side, z_Q is found as 60 using (7), where l is the number of layers.

The resultant motor parameters are shown in Table 2. In Fig. 5, the proposed winding diagram of one module is shown. The main purpose behind the selection is having large enough winding factor while keeping the space harmonic content low.

$$T_m = 2\,\sigma\,V_m = 2\,B_{avg}\,A_{rms}\,V_m \quad (1)$$

$$V_m = \pi\,{D_{is}}^2\,L_a/4 \quad (2)$$

$$E_{ph-m} = 4.44\,N_{ph-m}\,f_s\,\Phi_{pp}\,k_w \quad (3)$$

$$\Phi_{pp} = 2\,D_{is}\,L_a\,B_g/p \quad (4)$$

$$f_s = N_m\,p\,/120 \quad (5)$$

$$V_{ph-m} = m_a\,V_{dc-m}/2\sqrt{2} \quad (6)$$

$$z_Q = 2\,N_{ph-m}/w_s\,l \quad (7)$$

TABLE II
THE RESULTANT MOTOR PARAMETERS

Parameter	Value
Number of stator slots, Q_s	24
Number of rotor poles, p	20
Motor axial length, L_a	100 mm
Stator outer diameter, D_{os}	270 mm
Stator inner diameter, D_{is}	200 mm
Air gap length, l_g	1.5 mm
Magnet thickness, l_m	4.5 mm
Number of turns per coil side, z_Q	60
Stator fill factor, k_{cu}	0.6
Stator winding factor, k_{ws}	0.933

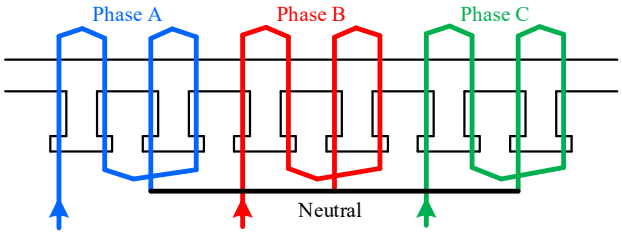

Fig. 5. Proposed winding diagram of one module

B. Design of the Drive

The selection of power semiconductor devices is based on voltage and current requirements. Among the suitable alternatives, motor drive efficiency is the main concern for device selection. The voltage requirement of each device has already been established. There are two GaN transistor types in the market which have breakdown voltage ratings as high as 650V, cascade GaNs manufactured by Transphorm and enhancement mode (e-mode) GaNs manufactured by GaN Systems [11]. The next step is to determine the current rating. By using the phase voltage calculated in the previous step, the phase current of each module can be found by using (8).

$$I_{ph-m} = P_{out-m} / \left[3\,\eta_m\,\cos(\varphi)\,f_s\,V_{ph-m}\right] \quad (8)$$

One device from each type is selected having similar ratings along with an IGBT for comparison purposes, as shown in Table 3 [11]. Power semiconductor device losses can be categorized as transistor forward conduction loss (P_{tc}), transistor switching loss (P_{ts}), transistor reverse conduction loss (anti-parallel diode conduction loss for IGBT case, P_{dc}) and loss on C_{oss} capacitance (P_{oss}) (or diode reverse recovery loss for IGBT case, P_{dr}). The analytical model used in the loss calculations is shown in (9)-(15). An approximate method which is well-established and commonly used for sinusoidal motor drive inverters is utilized to simplify the analysis. In this model, I_{cp} and I_{ep} are the forward and reverse peak currents, respectively, f_{sw} is the switching frequency, φ is the power factor angle, E_{on}, E_{off} and E_{oss} stand for turn-on, turn-off and C_{oss} energies, $V_{ce\text{-}sat}$ is saturation voltage drop for the IGBT, $R_{ds\text{-}on}$ is the on-state resistance for GaN, V_{ec} is the reverse voltage drop for the diode, I_{rr} and t_{rr} are the diode reverse recovery current and time, respectively, and $V_{ce\text{-}p}$ is the reverse recovery peak voltage.

$$P_{tc} = I_{cp}\,V_{ce-sat}\,[1/8 + m_a\cos(\varphi)/3\,\pi]\;(IGBT) \quad (9)$$

$$P_{tc} = {I_{dp}}^2\,R_{ds-on}\,[1/8 + m_a\cos(\varphi)/3\,\pi]\;(GaN) \quad (10)$$

$$P_{ts} = \left(E_{on} + E_{off}\right)[f_{sw}/\pi] \quad (11)$$

$$P_{dc} = I_{ep}\,V_{ec}\,[1/8 - m_a\cos(\varphi)/3\,\pi]\;(IGBT) \quad (12)$$

$$P_{dc} = {I_{sp}}^2\,R_{ds-on}\,[1/8 - m_a\cos(\varphi)/3\,\pi]\;(GaN) \quad (13)$$

$$P_{oss} = E_{oss}\;f_{sw}\,/\,\pi \quad (14)$$

$$P_{dr} = I_{rr}\,t_{rr}\,V_{ce-p}\,[f_{sw}/8] \quad (15)$$

TABLE III
ALTERNATIVE DEVICES FOR TRANSISTOR SELECTION [11]

Device	FP35R12KT4P	TPH3205WSB	GS66508B
Type	IGBT	Cascode GaN	E-mode GaN
Manufacturer	Infineon	Transphorm	GaN systems
Voltage	1200 V	650 V	650 V
Current	35 A	35 A	30 A
$V_{ce,sat}$	2,15 V	-	-
$R_{ds,on}$	-	60 mΩ	50 mΩ

Selection of the DC bus capacitors is performed for the designed system using metal film type capacitors. To be able to compare the IMMD design with a conventional motor drive in terms of power density, the same design procedure is also applied to the conventional system with IGBTs. The parameters affecting the capacitor selection are DC voltage (V_{dc}), capacitance requirement to meet the voltage ripple constraint (C_{dc}), the current requirement due to the RMS rating of capacitor bank current ripple ($I_{c,rms}$) and temperature rise of each capacitor (T_{core}). The analytical model used for these parameters are shown in (16)-(19), where $V_{dc\text{-}r}$ is the maximum allowed peak-to-peak voltage ripple in percent, T_a is the ambient temperature, P_c is the power loss on capacitor which is also dependent on core temperature, $R_{th\text{-}c}$ is the thermal resistance of the capacitor and R_c is the ESR value of the capacitors [6], [12].

$$C_{dc} = \frac{m_a\,I_{s,rms}}{16\,V_{dc-r}\,f_{sw}}\sqrt{\left(6 - \frac{96\sqrt{3}m_a}{5\pi} + \frac{9{m_a}^2}{2}\right)(\cos\varphi)^2 + \frac{8\sqrt{3}m_a}{5\pi}} \quad (16)$$

$$I_{c,rms} = I_{s,rms}\sqrt{2\,m_a\left(\frac{\sqrt{3}}{4\pi} + (\cos\varphi)^2\left(\frac{\sqrt{3}}{\pi} - \frac{9m_a}{16}\right)\right)} \quad (17)$$

$$T_{core} = T_a + P_c(T_{core})\,R_{th,c} \quad (18)$$

$$P_c = {I_{c,rms}}^2\,R_c(T_{core}) \quad (19)$$

IV. SIMULATION RESULTS

The performance of the motor is analyzed using ANSYS/Maxwell simulation environment. The analytical results are shown in Table 4 which have been obtained via the RMxprt tool of Maxwell. The designed motor is simulated using 2D FEM analysis tool to obtain transient characteristics. The phase induced voltage, currents and machine torque are presented in Figs. 6, 7 and 8, respectively. The flux density distribution over one module is shown in Fig. 9. The efficiency of the motor is close to the targeted value, however the fill factor is made a little higher than the expected value to achieve this, which is still acceptable for concentrated windings. The 3rd order harmonic content of the induced voltage is actually cancelled on the line-to-line voltage thanks to the star connection. The torque ripple and cogging torque values are also below specified limits.

TABLE IV
MOTOR SIMULATION RESULTS (RMXPRT)

Parameter	Value	Parameter	Value
$E_{ph\text{-}m}$	71 V rms	J_{rms}	5.8 A/mm^2
$I_{ph\text{-}m}$	12 A rms	P_{cu}	411 W
T_m	127 Nm	P_{core}	117 W
k_{cu}	68 %	η_m	93.8 %

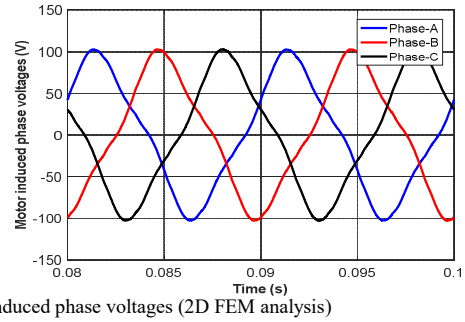

Fig. 6. Induced phase voltages (2D FEM analysis)

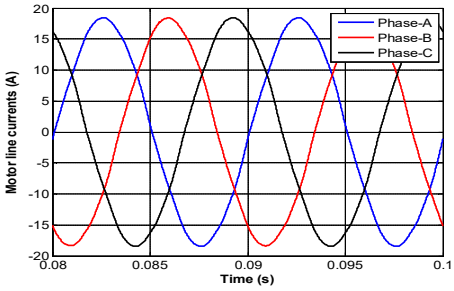

Fig. 7. Line currents of one module (2D FEM analysis)

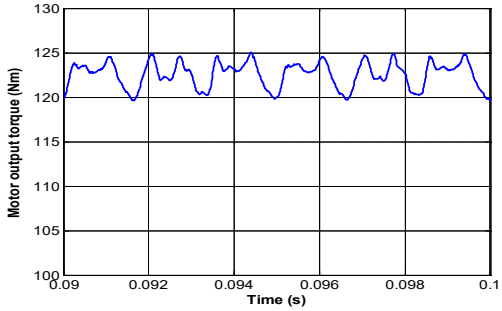

Fig. 8. Motor output torque (2D FEM analysis)

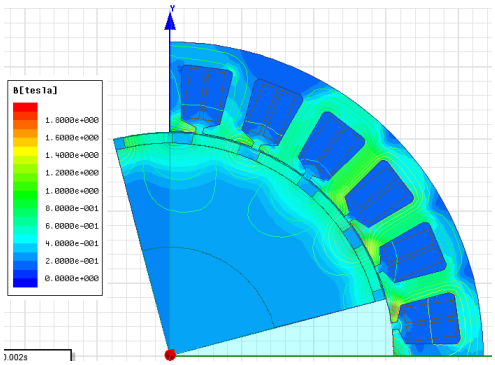

Fig. 9. Flux density distribution over one module

Loss analysis for the drive is performed using the presented model, which includes the selected devices with a conventional system having IGBTs and two IMMD systems with different types of GaNs. The comparative loss results are shown in Fig. 10. The results show that, even with a switching frequency five times the one with IGBTs, the total system loss is halved with GaN devices. The reason why 20 kHz is used for the system with IGBT is that, it is the practical limit for those devices. It is observed that the main reduction is on switching losses, as expected. However, transistor conduction losses are a little bit higher with GaNs, although reverse conduction losses are similar. There are two main reasons for this. First of all, IGBT conduction performance in high current applications is good. However, the GaN technology has not been proven itself in terms of on-state voltage drop, while it has developed to have comparable performance. Secondly, the IMMD system has 2-series structure so that each module carries two times the current they would have when there a 4 parallel modules. In conclusion, both cascade and e-mode GaN FETs reach 98% drive efficiency at 100 kHz switching frequency. Motor drive simulations are performed using 4 modules used with the proposed configuration, with 90^0 phase shift and suitable DC link capacitor which results in less than 1% voltage ripple. The DC link current of each parallel connected module and the total DC link current with and without interleaving at 50kHz switching frequency are shown in Fig. 11. The DC link voltage ripple of each series connected module and the total DC link voltage with and without interleaving are also shown in Fig. 12.

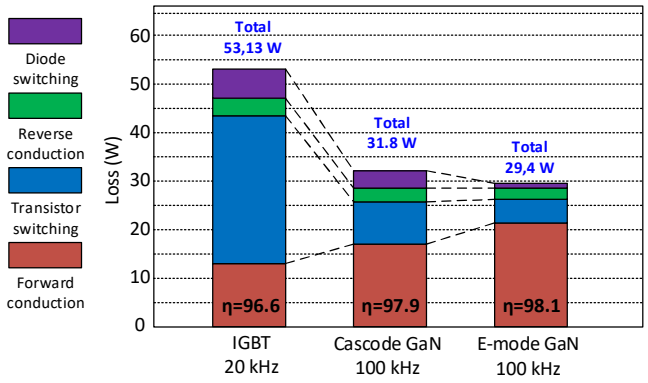

Fig. 10. Comparative loss analysis having a conventional system with IGBT and two different IMMD systems with GaN

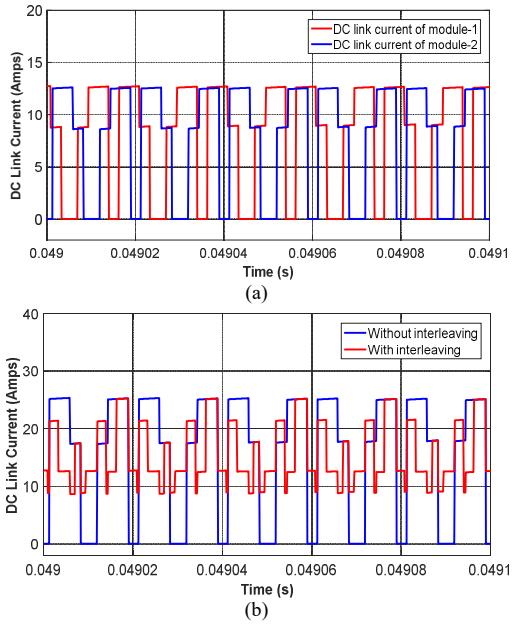

Fig. 11. (a) The DC link current of each module, (b) total DC link current with and without interleaving

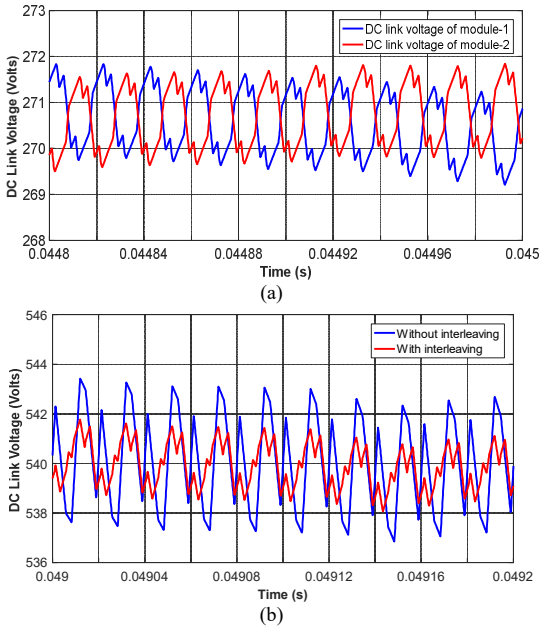

Fig. 12. (a) DC link voltage of each module, (b) Total DC link voltage with and without interleaving

The line-to-line output voltage and line current of one module are shown in Fig. 13. The performance of the proposed IMMD system and its conventional counterpart are listed in Table 4 including the RMS ripple current of each capacitor (I_{crms}), the required capacitance for each capacitor to meet the DC link voltage ripple constraint (C_{dc}), required voltage for each capacitor (V_c), number of total capacitors used, total harmonic distortion of the line-to-line voltage ($THDv$) and total harmonic distortion of the line current ($THDi$). In this analysis, switching frequencies used for IMMD is 50kHz and for the conventional motor drive is 20kHz.

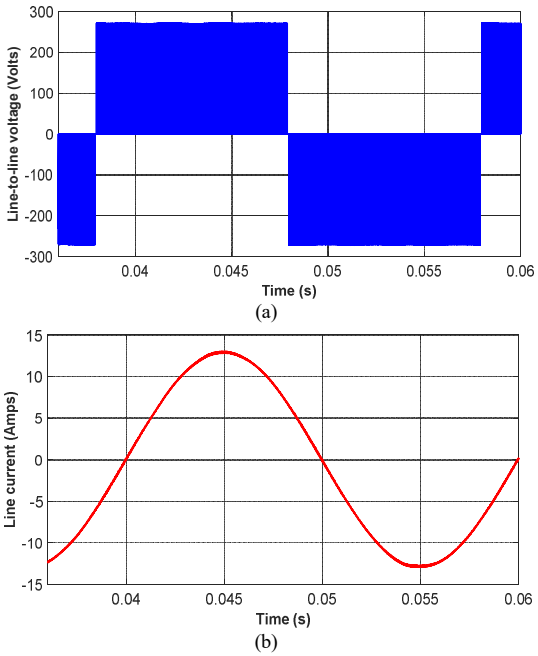

Figure 13. (a) Line-to-line voltage, (b) Line current

The results show that, the required RMS ripple current rating of the capacitors is decreased to almost half with the application of interleaving in the IMMD case. Metallized film capacitors are known to have high current handling capability, therefore decreasing the capacitance requirement is more critical and the most convenient way to achieve this is increasing the switching frequency. However, the current rating does not depend on the switching frequency and therefore it may be a deciding parameter for conventional motor drives. The capacitance requirement also decreases almost to its half with interleaving. It can also be reduced further with higher switching frequencies using GaN devices when IMMD configuration is used. One drawback of using the modular configuration is the necessity of using two capacitor banks due to the series connection. Interleaving between series connected modules does not contribute to any of the parameters id the DC link voltage ripple is to be kept below 1% for each module separately. On the other hand, the voltage of each capacitor is lower which decreases the size of the capacitor significantly.

For better visualization, capacitors from commercially available products are selected for the conventional and proposed systems, parameters of which are listed in Table 5. Using the thermal model, the temperature rise of the capacitors is also analyzed and shown in Table 5. Finally, the resultant power density of both the capacitor bank and overall IMMD is analyzed to verify the performance of the design. Using the motor dimensions, PCB dimensions and capacitor heights, the power density of the capacitor bank and overall system (excluding the heat sink) are found as 184 W/cm^3 and 1.1 W/cm^3, respectively. This result shows that, the performance criteria defined for the design process have been achieved in terms of power density, efficiency and reliability.

TABLE IV
PERFORMANCE OF THE PROPOSED IMMD AND COMPARISON WITH THE CONVENTIONAL SYSTEM

Parameter	Conventional System	Proposed System
$I_{c,rms}$	10.13 A	5.76 A
C_{dc}	97 µF	18 µF
V_c	630 V	300 V
Total capacitor	1	2
THDv	79.91 %	89.15 %
THDi	0.48 %	0. 47 %

TABLE V
PARAMETERS OF THE SELECTED CAPACITOR BANKS

Parameter	Conventional	Proposed
Voltage	600 V	300 V
Capacitance	100 µF	20 µF
Current	100 A	20 A
ESR	0.9 mΩ	4 mΩ
ESL	25 nH	11 nH
Width/Length	101mm x 101mm	28mm x 42mm
Height	40 mm	37 mm
Total volume	408 cm^3	43.5 cm^3
Thermal resistance	6.9 ^{0}C/W	12 ^{0}C/W
Power loss	92 mW	132 mW
Temperature rise	0.6 ^{0}C	1.6 ^{0}C

V. CONCLUSIONS

In this study, an integrated modular motor drive system is proposed which can replace conventional motor drive systems, and its design process is presented. The proposed system brings several advantages such as increased power density, enhanced fault tolerance and reliability, reduction in EMI problems and voltage stress across devices, and increased surface area for better cooling.

The design is based on 2-level inverter modules which can be connected in series and/or parallel on the DC link thanks to the modular structure. The number of series/parallel modules are established based on the reduction in the size of the DC link capacitor with proper interleaving angle, and the available device voltage and current ratings. Dimensioning of a PMSM having FSCW stator is performed and a suitable modular winding configuration is proposed. The design of the modular motor drive is based on WBG GaN power FETs selected from two different manufacturers. Loss characterization and analysis is performed using these devices along with a conventional converter in which IGBT is utilized for comparison.

It has been shown that both GaN devices yield superior efficiency performance even with a switching frequency five times the conventional one. Moreover, selection of DC bus capacitor banks is performed for these systems and the effects of interleaving, which is only applicable for modular structure, to the size of capacitors are presented. It is shown that, a power density higher than 1 kW/lt can be achieved with 98% motor drive efficiency for an IMMD having 8 kW output power. Considering also the improvements on the system reliability and fault tolerance, the performance of the IMMD system has been proven to be successful to replace the conventional motor drive systems using the design process presented here.

VI. ACKNOWLEDGMENT

This work is partially supported by Scientific and Technological Research Council of Turkey (TUBITAK) under the TUBITAK project number 117E252.

VII. REFERENCES

[1] R. Abebe et al., "Integrated motor drives: state of the art and future trends," *IET Electr. Power Appl.*, vol. 10, no. 8, pp. 757–771, Sep. 2016.

[2] J. J. Wolmarans, M. B. Gerber, H. Polinder, S. W. H. De Haan, J. A. Ferreira, and D. Clarenbach, "A 50kW integrated fault tolerant permanent magnet machine and motor drive," *PESC Rec. - IEEE Annu. Power Electron. Spec. Conf.*, pp. 345–351, 2008.

[3] M. D. Hennen, M. Niessen, C. Heyers, H. J. Brauer, and R. W. De Doncker, "Development and control of an integrated and distributed inverter for a fault tolerant five-phase switched reluctance traction drive," *IEEE Trans. Power Electron.*, vol. 27, no. 2, pp. 547–554, 2012.

[4] J. Wang, Y. Li, and Y. Han, "Integrated Modular Motor Drive Design With GaN Power FETs," *IEEE Trans. Ind. Appl.*, vol. 51, no. c, pp. 3198–3207, 2015.

[5] A. Shea and T. M. Jahns, "Hardware integration for an integrated modular motor drive including distributed control," in *2014 IEEE Energy Conversion Congress and Exposition (ECCE)*, 2014, pp. 4881–4887.

[6] M. Ugur and O. Keysan, "DC link capacitor optimization for integrated modular motor drives," *2017 IEEE 26th Int. Symp. Ind. Electron.*, vol. i, pp. 263–270, 2017.

[7] N. R. Brown, T. M. Jahns, and R. D. Lorenz, "Power Converter Design for an Integrated Modular Motor Drive," *Ind. Appl. Conf. 2007. 42nd IAS Annu. Meet. Conf. Rec. 2007 IEEE*, pp. 1322–1328, 2007.

[8] J. Wang and Y. Han, "A new concept of multilevel converter motor drive with modular design and split winding machine," in *2014 Power and Energy Conference at Illinois (PECI)*, 2014, pp. 1–6.

[9] S. U. Chung, J. M. Kim, D. H. Koo, B. C. Woo, D. K. Hong, and J. Y. Lee, "Fractional slot concentrated winding permanent magnet synchronous machine with consequent pole rotor for low speed direct drive," *IEEE Trans. Magn.*, vol. 48, no. 11, pp. 2965–2968, 2012.

[10] J. Wang, Y. Li, and Y. Han, "Evaluation and design for an integrated modular motor drive (IMMD) with GaN devices," *2013 IEEE Energy Convers. Congr. Expo. ECCE 2013*, no. Immd, pp. 4318–4325, 2013.

[11] E. A. Jones, F. F. Wang, and D. Costinett, "Review of Commercial GaN Power Devices and GaN-Based Converter Design Challenges," *IEEE J. Emerg. Sel. Top. Power Electron.*, vol. 4, no. 3, pp. 707–719, 2016.

[12] J. W. Kolar and S. D. Round, "Analytical calculation of the RMS current stress on the DC-link capacitor of voltage-PWM converter systems," *IEE Proc. - Electr. Power Appl.*, vol. 153, no. 4, p. 535, 2006.

VIII. BIOGRAPHIES

Mesut Uğur received his BSc and MSc degrees from the Department of Electrical and Electronics Engineering, Middle East Technical University, Ankara, Turkey in 2012 and 2015, respectively. He is currently working towards the PhD degree at Middle East Technical University.

He is currently a Research Associate in Middle East Technical University. His main research interest are electric motor drives, renewable energy and embedded systems.

Ozan Keysan received the M.S. degree from the Middle East Technical University, Ankara, Turkey, in 2008, and the Ph.D. degree investigating high-temperature superconducting direct-drive generators for offshore wind turbines at the Institute for Energy Systems at Edinburgh University, Edinburgh, U.K. in 2013.

He is currently an Assistant Professor in Middle East Technical University. His research interests include renewable energy, design and optimization of electrical machines and smart grids.